

# Silver nanoparticles dispersed in polyimide thin film matrix

M.E. Fragalà<sup>1,a</sup>, G. Compagnini<sup>1</sup>, G. Malandrino<sup>1</sup>, C. Spinella<sup>2</sup>, and O. Puglisi<sup>1</sup>

<sup>1</sup>Dipartimento di Scienze Chimiche dell'Università di Catania, Viale Andrea Doria, 6, I-95125 Catania, Italy

<sup>2</sup>CNR-IMETEM, Stradale Primosole, 50, I-95121 Catania, Italy

Received: 1 September 1998 / Received in final form: 5 November 1998

**Abstract.** A new metallorganic silver precursor, Ag(hfa)tetraglyme, has been used to produce silver aggregates into polymeric thin film matrices by thermal reduction in a temperature range between 200 °C and 300 °C. Here we present a characterization of the metal aggregates into polyimide thin films (0.1–1 μm). The size of the metallic particles has been measured by transmission electron microscopy (TEM). A narrow particles size distribution centered around a radius value of ~16 nm has been observed. X-ray diffraction (XRD) performed on this sample confirms the presence of metallic silver. X-ray photoelectron spectroscopy (XPS) has been used to determine the elemental composition at the particle surface. A partial oxidation of the metal particles, probably due to the air contamination or to interaction with oxygen of the polymeric matrix, has been observed.

**PACS.** 72.80.G Transition metal compounds – 71.20.Rv Polymers – 82.30.N Cluster formation in chemical reactions

## 1 Introduction

Nanoscale materials are widely studied because the effects of confinement and quantization of electrons in a reduced volume can affect optical, electronic, and chemical properties of this kind of material [1, 2]. Noble metal nanoparticles have been produced by different methods [3–14] such as sol-gel, chemical synthesis, sputtering, electrochemical deposition, and low-energy cluster beam deposition (LEBCD). The main goal of these production techniques is the formation of very small aggregates and the control of their size to tailor their properties [5, 15]. Matrices having different natures can be used to limit the particles' dimensions by preventing their agglomeration through the decrease in diffusion of metal particles. Polymers can be used as matrices even if the synthesis of these polymer/metal materials is not largely used [16, 17], mainly because the synthetic procedures involved might present difficulties due to the low mutual solubility of the two components. In this work, a new metallorganic silver complex, Ag(hfa)tetraglyme, is used as a precursor of metallic silver particles. A polyamic acid (PAA) precursor has been chosen because it transforms in polyimide (PI) at a curing temperature compatible with the metallorganic precursor reduction temperature, so that at the same time the precursor decomposes, giving metallic silver particles, and the PAA transforms itself in PI, allowing the silver particles to remain trapped in the polymeric cage. Different techniques (X-ray Photoelectron Spectroscopy (XPS),

X-ray Diffraction (XRD) and Transmission Electron Spectroscopy (TEM)) have been used to characterize the system of polyimide–silver particles, in order to study the surface (XPS) and the bulk (XRD) of the system and to confirm the presence of nanoparticles inside the polymeric film (TEM).

## 2 Experimental

The metallorganic silver compound has been synthesized from a tetrahydrofuran (THF) suspension of Ag<sub>2</sub>O, at which two coordination ligands have been added, the tetraethylen-glycol-dimethylether, CH<sub>3</sub>(OCH<sub>2</sub>CH<sub>2</sub>)<sub>4</sub>OCH<sub>3</sub> and the 1,1,1,5,5,5-hexafluoro-2,4-pentandione (Hhfa). A new complex having the formula Ag(hfa)(tetraglyme) is produced; this has been confirmed by several analysis techniques, such as mass spectrometry, which has revealed the presence of typical fragmentation patterns, differential scanning calorimetry, by which the fusion temperature of the complex has been determined ( $T_f = 42$  °C), elemental analysis, and X-ray photoelectron spectroscopy (XPS). Thermogravimetric analysis (TGA) describes the thermal decomposition of the precursor that starts at  $T = 130$  °C, with a maximum yield at  $T = 200$  °C. In this temperature range, thermal reduction of the compound, producing metallic silver, takes place. The Ag(hfa)(tetraglyme) solubility is exploited to mix this precursor with a polyamic acid (PAA), PIQ-L100 (polyimide-isoidroquinazoline-dione), in a *n*-methylpyrrolidone (NMP) solution. The weight concentration of silver in the PAA solution is about

<sup>a</sup> e-mail: mfragala@dipchi.unict.it

0.1%. This solution is then deposited by spin coating on a silicon substrate, and a thin film ( $\sim 1 \mu\text{m}$ ) is obtained in which both PAA and Ag(hfa)tetraglyme are contained. Knowledge of the thermal behavior of both the solution components suggests a thermal treatment at  $T = 300^\circ\text{C}$  for 1 h, so that thermal decomposition of the precursor can be obtained while the PAA $\rightarrow$ PI curing reaction takes place. XRD and XPS analysis of the obtained sample is used to determine the elemental composition of the surface. TEM analysis is performed to estimate the particles presence and their dimensions.

### 3 Results

Thin film of pure Ag(hfa)tetraglyme, obtained by the spin coating of a  $\text{CHCl}_3$  solution on a silicon substrate, can be thermally decomposed at  $T = 200^\circ\text{C}$ . In this way, one gets a film with grain dimension of 100–300 nm, as revealed by scanning electron microscopy (SEM), not shown here. The silver precursor has been decomposed inside the polyamic acid PIQ-L100 to reduce the aggregates' dimensions. During the thermal annealing at  $T = 300^\circ\text{C}$ , the density of the polymeric matrix changes as it goes from PAA to PI: in fact, as the curing reaction takes place, the formation of the imide rings causes an increase of the rigidity of the polymeric system. Silver particles embedded in the cured PIQ are smaller with respect to the dimensions of the silver grains detected in the thermally treated Ag(hfa)tetraglyme film previously described. In Fig. 1a is reported the TEM image (planar view) of the PI film, in which discrete nanoparticles are homogeneously distributed inside the polymeric matrix, showing a narrow size distribution ( $\sigma = 1.2 \text{ nm}$ ) centered at a radius value of 16 nm (Fig. 1b). In order to determine the chemical state of the silver particles detected inside the polymeric film, an XRD analysis has been performed. In Fig. 2 is shown the diffractogram, in which typical metallic silver peaks are present. In particular, the strongest one corresponds to the most intense (100%) silver (111) diffraction ( $2\theta = 38.1^\circ$ ), while the two less intense peaks are associated to the (200) diffraction ( $2\theta = 44.36^\circ$ ) and to (311) diffraction ( $2\theta = 77.54^\circ$ ), respectively. The grazing incident angle X-ray diffraction (GID) has also revealed the less intense (27%) (220) diffraction ( $2\theta = 64.17^\circ$ ) of the metallic silver. The arrow in the figure indicates the position of the strongest reflection of  $\text{Ag}_2\text{O}$ . As one can see, no appreciable amount of silver oxide can be detected. The surface elemental composition of the samples is provided by XPS. In Fig. 3 is shown the valence band (VB) of the silver particles embedded in a cured PIQ matrix, which suggests the presence of some form of oxidized silver. In particular, the narrowing of the valence band (VB) of the Ag in PIQ and the disappearing of the shoulder at high binding energy are correlated to the loss of the 5s-type orbital contribution to the silver Density of States (DOS) [18], because of the formation of  $\text{Ag}^+$  ions. Therefore an oxygen interaction with metallic silver particles is detected by XPS analysis; this is confirmed by other evidence, such as a broadening

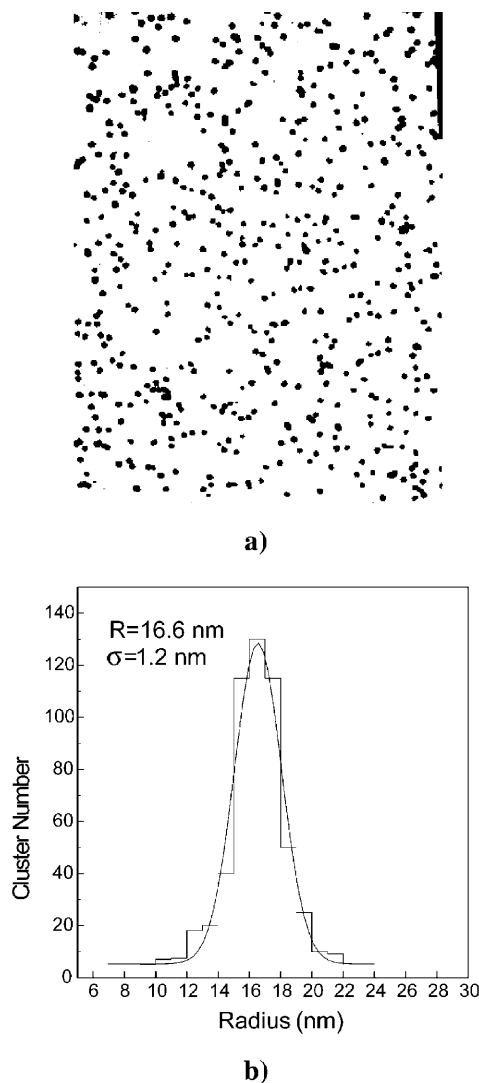


**Fig. 1.** (a) TEM image (planar view) of the PIQ/Ag particle film. The dark particles are the silver particles inside the polyimide matrix. (b) Size distribution of the silver particles detected by TEM. It is centered around a mean value of 16.6 nm ( $\sigma = 1.2 \text{ nm}$ ).

of both  $\text{Ag}3d$  peaks (3/2 and 5/2) of the PIQ/Ag particle film (FWHM = 1.6 eV) with respect to those of a silver foil taken as reference sample (FWHM = 1.1 eV) that can be also ascribed to an oxidation of the silver particles [19–22]. This result seems to be in contrast with the XRD results, which did not show any silver oxide diffraction peak. This contrast can be resolved by considering the different sampling depth of the two characterization techniques: XRD is in fact a bulk technique, while XPS is a surface technique characterized by a sampling depth of 20 Å for silver and 34 Å for PIQ [23]. This can explain why only the silver oxide cluster skin is detected by XPS, while the XRD cannot reveal this negligible contribution. In other words, combining XRD and XPS information, we can conclude that the particles observed in our PI film are mainly composed of pure metallic silver, while their surface is charac-

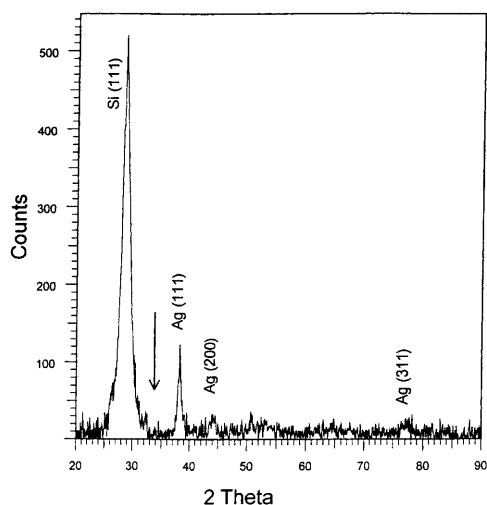


**Fig. 2.** XRD analysis of the PIQ/Ag particle film. The most intense peak is related to the silicon (111) substrate contribution. The other peaks are due to the diffractions of the metallic silver ( $\text{Ag}^0$ ). In the figure is also indicated the position of the most intense peak of silver oxide,  $\text{Ag}_2\text{O}$  (not detectable in our sample).

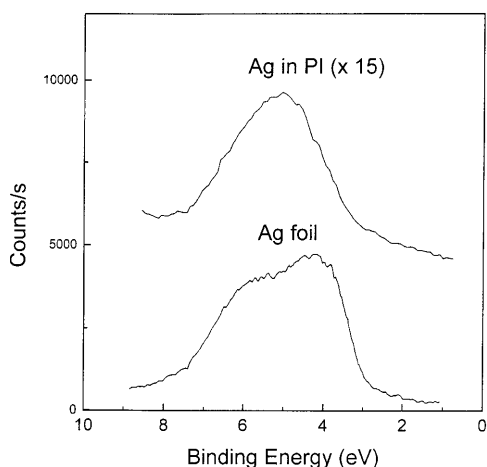


**Fig. 3.** Valence band (VB) of the PIQ/Ag particle film and of a silver foil taken as reference. For a better comparison the VB of the former is multiplied by an arbitrary factor.

terized by some chemical interaction with oxygen, regarding either atmospheric  $\text{O}_2$ , to give true  $\text{Ag}_2\text{O}$  phase on the cluster skin, or a chemical interaction between border Ag atoms and the oxygen of the polymeric matrix.

## 4 Conclusions

A method to produce silver particles of nanometric dimension inside a polyimide matrix, starting from a new metallorganic silver precursor, is reported. A narrow cluster size distribution having a mean radius of 16 nm is detected by TEM analysis performed on these samples. The XPS results show chemical interaction between silver particles

and oxygen atoms, as confirmed by the absence of the 5s contribution in the valence band presented here and also by the shape and position of the most representative photoelectron and Auger peaks, which for the sake of brevity are not shown in this paper (these results will be shown elsewhere). The oxygen interaction affects the cluster surface only, according to the XRD, which does not show any Ag oxide diffraction contribution.

The authors thank Professor Francesco Castelli for the thermogravimetric analysis of the samples. CNR (Rome) and MURST are gratefully acknowledged for financial support.

## References

1. F. Hoche, D. Ricard, C. Flytzanis: *J. Opt. Soc. Am. B* **3**, 1647 (1986)
2. O. Stenzel, R. Petrich: *J. Phys. D* **28**, 978 (1995)
3. A. Taleb, C. Petit, M.P. Pileni: *J. Phys. Chem. B* **102**, 2214 (1998)
4. J.M. Petroski, Z.L. Wang, T.C. Green, M.A. El Sayed: *J. Phys. Chem. B* **102**, 3316 (1998)
5. B. Palpant, B. Prével, J. Lermé, E. Cottocin, M. Pellarin, M. Trailleux, A. Perez, J.L. Vialle, M. Broyer: *Phys. Rev. B* **57**, 1963 (1998)
6. M. Lee, T.S. Kim, Y.S. Choi: *J. Non-Cryst. Solids* **211**, 143 (1997)
7. A. Martino, S.A. Yamonoka, J.S. Kawada, D.A. Loy: *Chem. Mater.* **9**, 423 (1997)
8. Y. Hasoya, T. Suga, T. Yanogawa, Y. Karokawa: *J. Appl. Phys.* **81**, 1475 (1997)
9. M.M. Alvarez, J.T. Khoury, T.G. Schaaff, M.N. Shafiqullin, I. Vezmar, R.L. Whellen: *J. Phys. Chem. B* **101**, 3706 (1997)
10. S. Fedrigo, W. Harbich, J. Buttlet: *Phys. Rev. B* **47**, 10706 (1993)
11. H. Ishikawa, T. Ida, K. Kimura: *Surf. Rev. Lett.* **3**, 1153 (1996)
12. J.A. Sawichi, G. Abouchara, J.A. Serughetti, A. Perez: *Nucl. Instrum. Methods B* **101**, 1548 (1997)
13. G.L. Hornyak, C.J. Patrissi, C.R. Martin: *J. Phys. Chem B* **101**, 1548 (1997)
14. A. Perez, P. Melinon, V. Depuis, P. Jensen, B. Prével, J. Tuillon, L. Bardotti, C. Martet, M. Trailleux, M. Broyer, M. Pellarin, J.L. Vialle, B. Palpant, J. Lermé: *J. Phys. D* **30**, 709 (1997)
15. A. Taleb, C. Petit, M.P. Pileni: *J. Phys. Chem. B* **102**, 2214 (1998)
16. Y.N.C. Chan, G.S.W. Craig, R.R. Schrock, R.E. Cohen: *Chem. Mater.* **4**, 885 (1998)
17. Y. Yuan, J.H. Fendler, I. Cabasso: *Chem. Mater.* **4**, 312 (1992)
18. G. Schon: *Acta Chem. Scand.* **27**, 2623 (1973)
19. J.S. Hammond, S.W. Gaarenstroom, N. Winograd: *Anal. Chem.* **47**, 2193 (1975)
20. V.K. Kaushik: *J. Electron Spectrosc. Relat. Phenom.* **56**, 273 (1991)
21. S.W. Gaarenstroom, N.J. Winograd: *J. Chem. Phys.* **67**, 15 (1977)
22. C. Rehren, M. Muhler, X. Bao, R. Schlog, G. Ertl: *Z. Phys. Chem.* **11**, 174 (1991)
23. M.P. Seah, W.A. Dench: *Surf. Interface Anal.* **1**, 1 (1979)